Materials and Design 30 (2009) 3913–3919

Contents lists available at ScienceDirect

Materials and Design

journal homepage: www.elsevier.com/locate/matdes

Short Communication

Effect of tool geometry on microstructure and mechanical properties of friction stir lap welded magnesium alloy and steel

Y.C. Chen *, K. Nakata

Joining and Welding Research Institute, Osaka University, 11-1 Mihogaoka, Ibaraki, Osaka 567-0047, Japan

ARTICLE INFO

Article history:
Received 18 January 2009
Accepted 6 March 2009
Available online 13 March 2009

ABSTRACT

The effect of tool geometry on microstructure and mechanical properties of friction stir lap welded AZ31 Mg alloy (top sheet) and steel (zinc coated steel and brushed finish steel) sheets was studied. Tools with two different probe lengths were used in this study. The microstructure at the joining interface, the failure loads and the fracture locations of the joints varied significantly with the probe length. For zinc coated steel joints, the short probe contributed to defect-free joints and high-strength joints; for brushed finish steel joints, long probe improved significantly the failure loads of the joints. The joints welded using a long probe fractured at the stir zone of magnesium alloy side while those welded using short probe fractured at the joining interface.

1. Introduction

Magnesium alloys with low density and high specific strength are being considered for fabrication of vehicles. Steels as the most common materials of modern industry account for the majority of the welded products. The use of the lap joining of magnesium alloy and steel in fabrication of vehicles can reduce the weight of automotive body. Therefore, the development of reliable joints between magnesium alloy and steel is required. From Mg–Fe binary alloy phase diagram we can know that the maximum solid solubility of Fe in Mg is 0.00041 at.%. It means that magnesium and steel do not mix in the liquid state at ambient pressure [1]. The melting points of Mg and Fe are 649 °C and 1538 °C, respectively. The great difference in the melting points between these two kinds of metals poses the difficulty in melting them at the same time during fusion welding. Moreover, they do not react with each other. Therefore, joining Mg alloys to steels by conventional fusion welding processes is very difficult.

As a solid-state welding technology, friction stir welding (FSW) process [2] can weld Mg alloys [3–7] and steel [8–15] and get high quality joints compared with fusion welding technology. It is also possible to produce good welds when FSW is used to join dissimilar materials of magnesium alloys and steels. Watanabe et al. [16] studied the weldability of FSW AZ31 magnesium alloy/SS400 steel, and reported that the rotation speed and the position of the pin axis had a significant effect on the strength and the microstructure of the joint. The maximum tensile strength of a butt joint reached about 70% of that of the magnesium base metal. It is well known that the formation of FSW zone is affected by the material flow behavior under the action of FSW tool. That is to say, the material plastic flow behavior and the heat generation are predominantly influenced by the FSW tool profiles and FSW tool dimensions when FSW process parameters are fixed. Up to date, a few studies about the effect of tool geometry on the microstructure evolution and mechanical properties in FSW of aluminum alloys have been reported [17–20].

In the present study, 1.6-mm-thick AZ31 magnesium alloy and 0.8-mm-thick steel sheets of two kinds (zinc coated steel and brushed finish steel) are selected as the experimental materials for friction stir lap welding. The magnesium alloy sheet is put on the steel sheet. Two different probe lengths (1.5 mm and 1.8 mm) are used in this study. For 1.5-mm-length probe, the probe tip of the tool does not touch the surface of the steel sheet during welding. For 1.8-mm-length probe, the probe tip of the tool is inserted into the lower steel sheet during FSW. The tensile strengths, fracture locations and microstructural features in the lap interface are examined and the effects of tool probe length on the microstructure at the joining interface, the failure loads and fracture locations of the joints are discussed.

2. Experimental procedure

The base materials used in this study were a 1.6-mm-thick AZ31 magnesium alloy sheet and a 0.8-mm-thick low carbon steel sheet. For comparison, two kinds of steel sheets were selected, i.e., zinc coated steel and brushed finish steel. The chemical composition and mechanical properties of the base materials are shown in Table 1. Rectangular welding samples, 300 mm long by 100 mm wide, were lap welded using a FSW machine. A graphic scheme of the FSW process was shown in Fig. 1. The welding parameters were rotation speed of 25 rad s^{-1} and welding speed

* Corresponding author. Tel./fax: +81 6 6879 8668.
E-mail address: armstrong@hit.edu.cn (Y.C. Chen).

0261-3069/$ - see front matter © 2009 Elsevier Ltd. All rights reserved.
doi:10.1016/j.matdes.2009.03.007

Table 1
Chemical compositions and mechanical properties of base materials.

Base materials	Chemical compositions (mass%)										Mechanical properties	
	Al	Cu	Mn	Fe	C	Mg	Ni	P	Zn	S	Strength (MPa)	Elongation (%)
AZ31	3	–	0.2	–	–	Bal.	–	–	1	–	239	13
Zn coated steel	0.06	0.02	0.20	Bal.	0.04	–	0.01	0.013	–	0.005	328	33.4

of 1.67–5 mm s^{-1}. The upsetting force of the welding tool (made of SKD61 tool steel) was 3.92 kN. The shoulder diameter and probe diameter of the tool were 15 mm and 5 mm, respectively. The length of the probe was 1.5 mm and 1.8 mm. The welding tilt angle was 3°.

After welding, the joint was cross-sectioned perpendicular to the welding direction for the metallographic analysis and tensile tests using an electrical-discharge cutting machine. The cross-sections of the metallographic specimens were mechanically ground with water abrasive paper and polished with 3 μm and 1 μm diamond, and observed by optical microscopy (OM). The mechanical properties of the joint were measured using tensile tests. The tensile tests were carried out at room temperature at a crosshead speed of 0.0167 mm s^{-1} using a tensile testing machine, and the mechanical properties of the joint were evaluated using three tensile specimens cutting from the same joint. The shape of the test specimen was rectangular and the width of each specimen was 20 mm.

The welding thermal cycle histories along the interface during FSW were measured with an array of K-type thermocouples (0.2 mm diameter) at various locations from the weld center. Microstructure characteristic and element distribution along the interface were analyzed by scanning electron microscopy (SEM) equipped with an energy-dispersive X-ray spectroscopy (EDS) analysis system. Fracture surfaces of joints were analyzed using X-ray diffraction (XRD) after tensile test.

3. Experimental results

Figs. 2 and 3 show the effect of probe length on the tensile strengths and fracture locations of lap joints of AZ31 magnesium alloy with two kinds of steels. Tensile test results show that the probe length has a significant effect on the mechanical properties of lap joints welded at the same welding parameters. For brushed finish steel joints, the failure loads of the joints increase significantly with the increasing probe length. For example, the joints welded using 1.5-mm-length probe split in the preparation of the tensile test samples when the welding speed is higher than 3.33 mm s^{-1}. In contrast the joints welded using 1.8-mm-length probe show relatively high failure loads. For zinc coated steel joints, the failure loads of the two kinds of joints show a similar result, which means the increase of the probe length does not significantly improve the tensile strength. The results of the fracture locations show that whether brushed finish steel joints or zinc coated steel joints, all the joints welded using a 1.8-mm-length probe fracture at the stir zone of magnesium alloy side while those welded using a 1.5-mm-length probe fracture at the joining interface. It indicates that the weakest part of the joints moves from the joining interface to the stir zone of magnesium alloy side when increasing the probe length of the tool.

The macroscopic view of traverse section of zinc coated steel joints and brush finished steel joints welded using the 1.5-mm-length probe and the 1.8-mm-lengh probe are shown in Fig. 4. It can be seen from these figures that magnesium alloy and steel are joined tightly and the microstructure characteristic in magnesium alloy side is similar to that of friction stir welded magnesium alloy itself. For the joints welded using the 1.5-mm-length probe, stir zone (SZ) is only in Mg alloy side; for the joints welded using the 1.8-mm-length probe, SZ has extended to steel side. In this study, we are mainly interested in the interface structure feature. Microstructure is observed in the region from the center of the weld to the base material. The typical details of the microstructural variations from position A to position G are demonstrated in Figs. 5 and 6. Figs. 7 and 8 show SEM and EDS (line scanning analysis along the dotted line) analysis results vertical to the interface of two kinds of joints welded using the 1.5-mm-length and the 1.8-mm-length probe.

Figs. 5a and 7a show the microstructure at the center of lap interface (position A shown in Fig. 4a) of zinc coated steel joints welded using the 1.5-mm-length probe. It can be seen from Fig. 5a that the structure of the joint consists of three layers, i.e., microstructure in SZ of magnesium alloy, an intermetallic compound (IMC) layer and base material (BM) of steel. The representative concentration profiles of Mg, Zn, Al and Fe cross the interface between magnesium alloy and steel are shown in Fig. 8a. Zn is not detected and Al is rich. The result suggests that IMC of Al/Mg or Al/

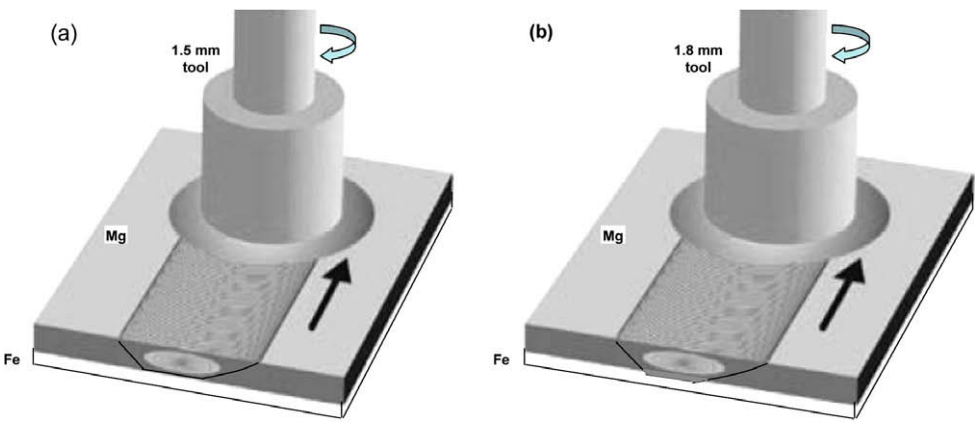

Fig. 1. A graphic scheme of the FSW process.

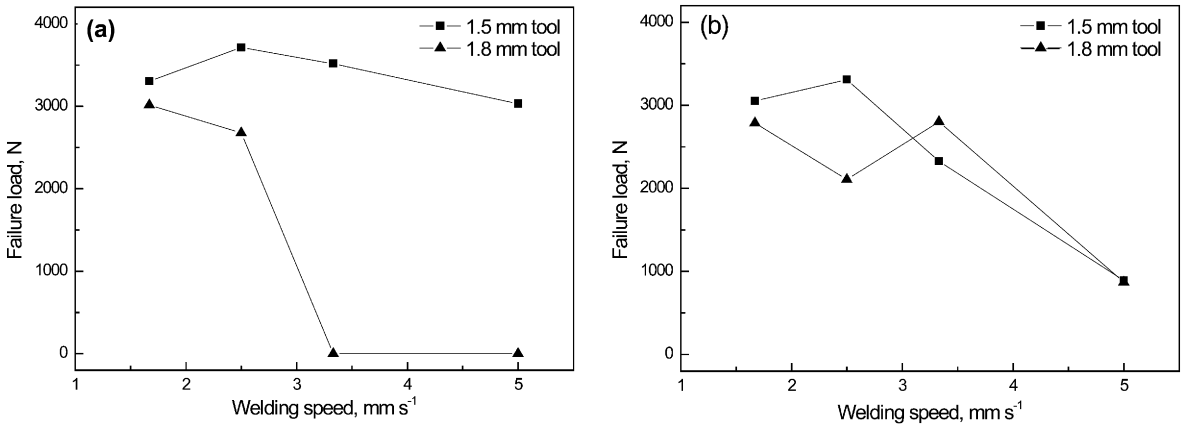

Fig. 2. Effect of tool geometries on the tensile strength of the joints: (a) brush finished steel joints; (b) zinc coated steel joints.

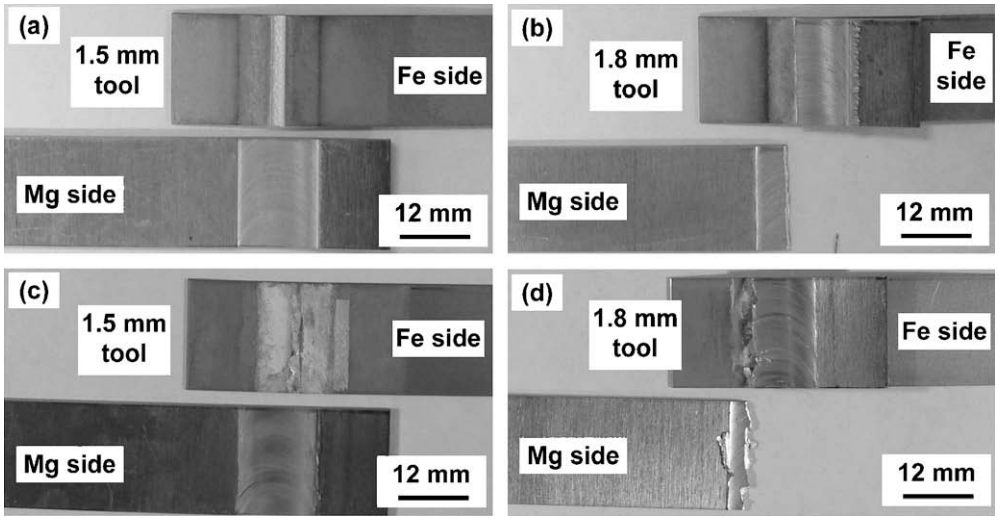

Fig. 3. Effect of tool geometries on the fracture locations of the joints: (a, b) brush finished steel joints; (c, d) zinc coated steel joints.

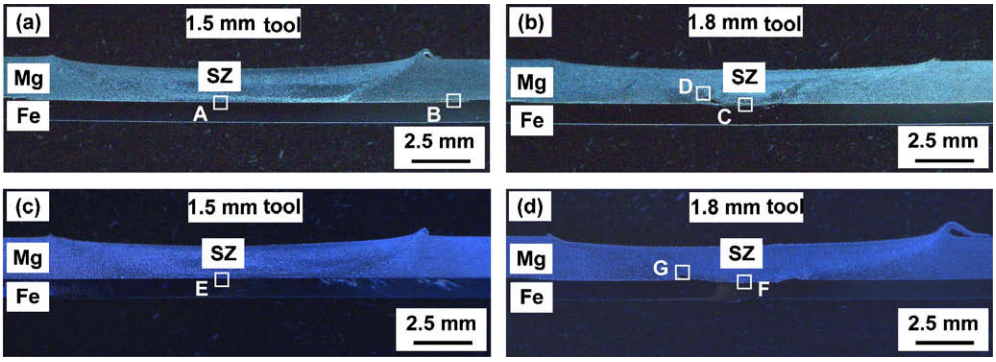

Fig. 4. Cross-sections of the joints: (a, b) zinc coated steel joints; (c, d) brush finished steel joints.

Fe possibly forms at the bonding interface. Fig. 5b shows the microstructure at position B in Fig. 4a. It seems that this zone has a solidified microstructure. The solidified structure fills into the clearance between magnesium alloy and zinc coated steel. As shown in Fig. 4a, this position has slightly exceeded the domain of shoulder diameter of the tool. Quantitative analysis of the chemical compositions by EDS shows that the white massive phase consists of 76.16 at.% Mg, 11.3 at.% O and 12.55 at.% Zn, while the grey substrate contains 64.13 at.% Mg, 4.47 at.% O and 31.41 at.% Zn. It suggests that the white phase is primary phase of Mg and the grey substrate is Mg_7Zn_3. Meanwhile, this zone shows an apparent O-rich characteristic. It suggests that liquid eutectic structure with O-rich products flows to this position during FSW. Figs. 5c and 7b show the microstructure at the interface center (position C in Fig. 4b) of the joint welded using the 1.8-mm-length probe. The representative concentration profiles of Mg, Zn, Al and Fe cross

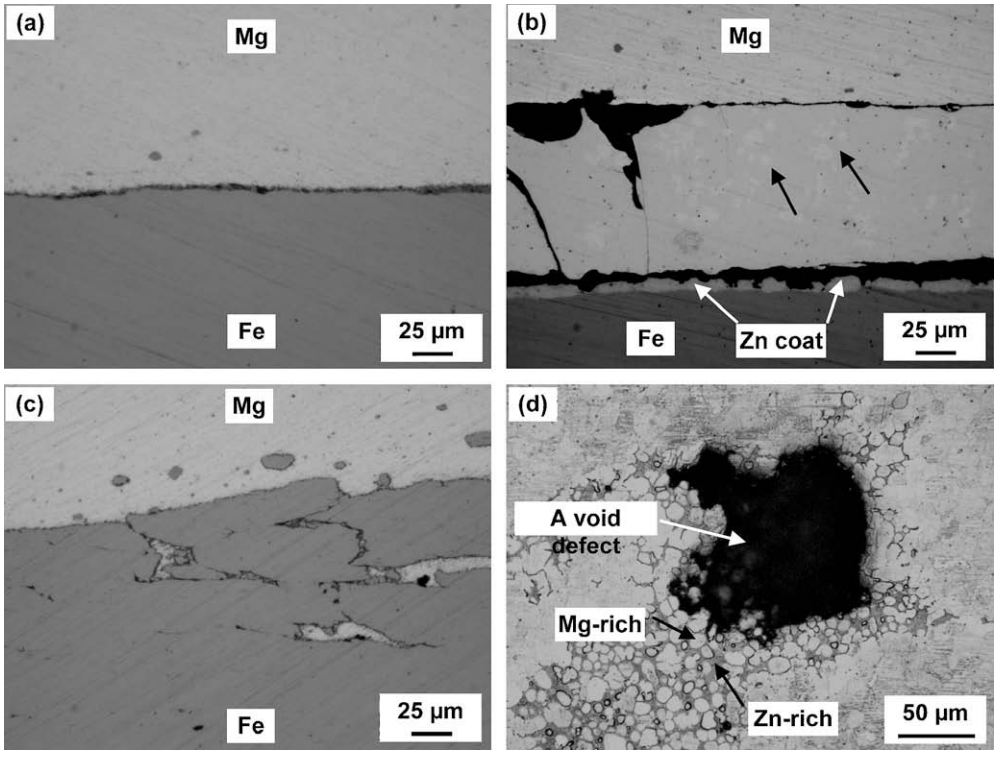

Fig. 5. OM micrographs of different positions shown in Fig. 4a and b: (a) position A; (b) position B; (c) position C and (d) position D.

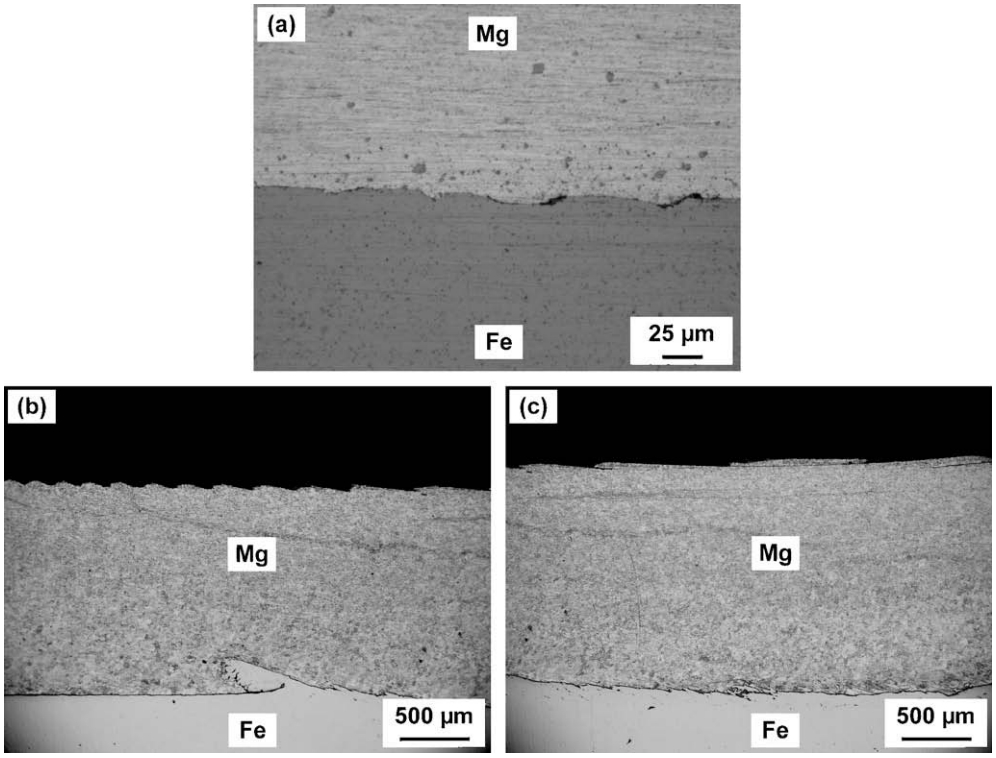

Fig. 6. OM micrographs of different positions shown in Fig. 4c and d: (a) position E; (b) position F and (c) position G.

the interface are shown in Fig. 8b. The SZ near the interface exhibits that a mixture of Mg and steel particles was pulled away by the forge of tool probe. Steel particles have an irregular shape and inhomogeneous distribution within SZ. Compared with the interface microstructure of the joint welded using the 1.5-mm-length probe, the interface of the joint welded using the 1.8-mm-length probe shows a thin interface structure of Mg and steel instead of a heavy IMC layer. Fig. 5d shows the microstructure at position D

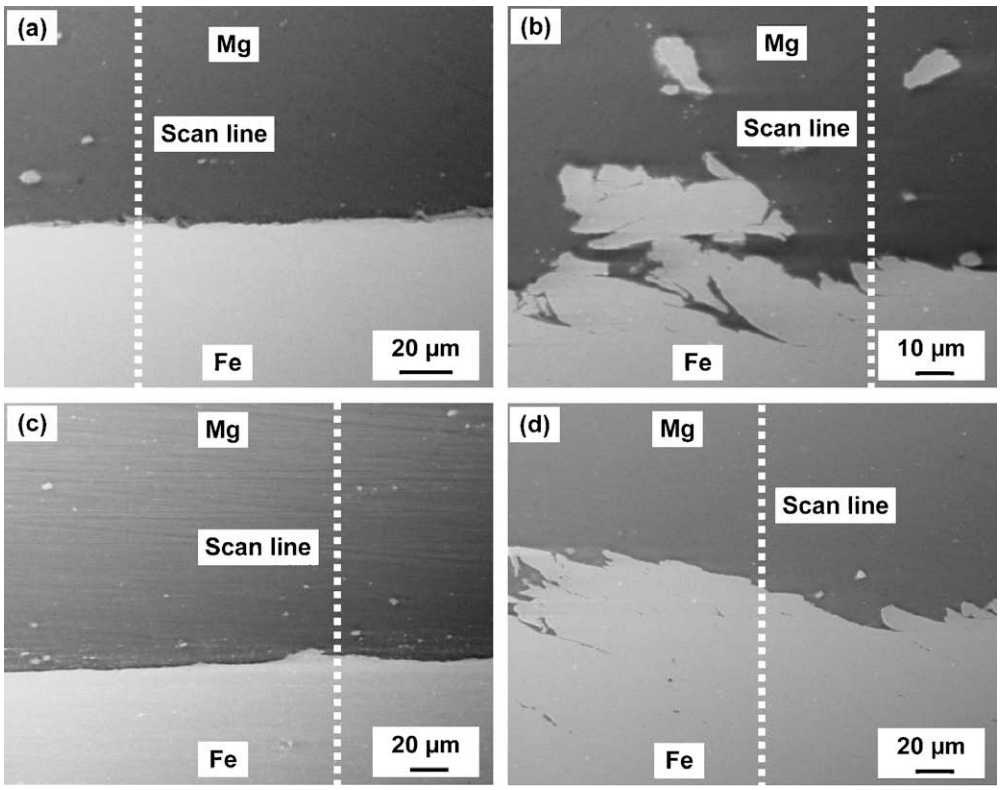

Fig. 7. SEM micrographs of different positions shown in Fig. 4: (a) position A; (b) position C; (c) position E and (d) position F.

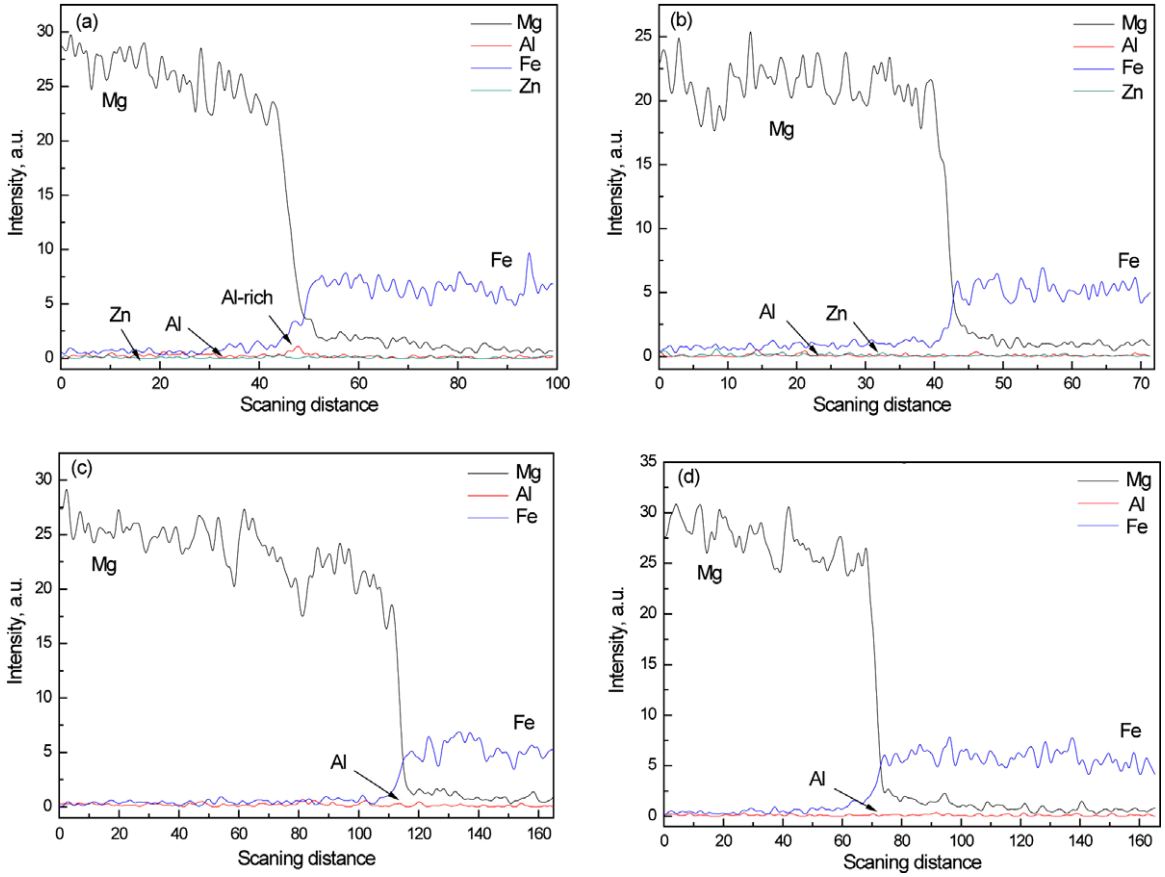

Fig. 8. EDS analysis results along the scan lines shown in Fig. 7: (a) along the scan line shown in Fig. 7a; (b) along the scan line shown in Fig. 7b; (c) along the scan line shown in Fig. 7c and (d) along the scan line shown in Fig. 7d.

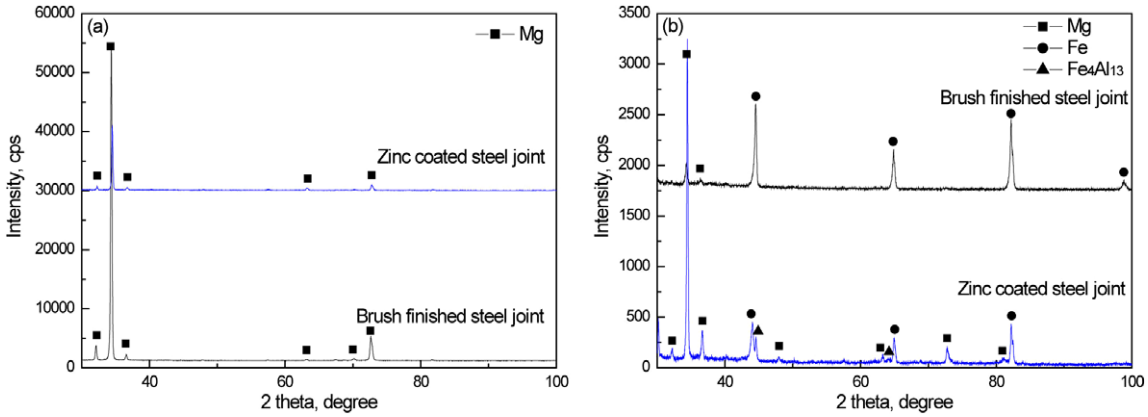

Fig. 9. XRD analysis results from the fracture surface of the joints welded using 1.5-mm-length probe (3.33 mm s^{-1}): (a) from Mg side of the joints and (b) from Fe side of the joints.

in Fig. 4b. This position is in the SZ and void defect is detected in this region. Quantitative analysis of the chemical compositions by EDS shows that Zn-rich region is detected. It suggests that liquid Mg–Zn eutectic structure occurred in this region during FSW. The presence of liquid phase leads to the formation of void defect.

Figs. 6a and 7c show microstructure at the center of lap interface of brushed finish steel joints welded using the 1.5-mm-length probe. The representative concentration profiles of Mg, Al and Fe cross the interface are shown in Fig. 8c. It can be seen that no significant IMC layer is found at the interface. Magnesium metal is pushed into the concavities of the brushed finish steel surface. Magnesium alloy and steel are joined through certain kind of mechanical bonding. Figs. 6b, c and 7d show the microstructure at the interface (position F and G in Fig. 4d) of the joint welded using the 1.8-mm-length probe. The representative concentration profiles of Mg, Zn, Al and Fe cross the interface are shown in Fig. 8d. Magnesium alloy and steel are joined tightly and the interface shows a thin interface structure.

In order to determine whether IMC forms at the interface or not, X-ray diffraction patterns from fractured surfaces of the joints welded using the 1.5-mm-length probe are analyzed. XRD analysis results are shown in Fig. 9. For zinc coated steel joints, diffraction lines from IMC of Fe_4Al_{13} are detected at steel side. At the same time, phases of Mg and Fe from base materials are also detected. For brushed finish steel joints, only phases of Mg and Fe are detected. This result indicates that in current experimental conditions no IMC forms at the interface when the brushed finish steel is selected as base material. The joining mechanism between magnesium alloy and brushed finish steel is mechanical bonding. XRD analysis for the joints welded using the 1.8-mm-length probe is not carried out because all the joints do not fracture at the interface. But the SEM and EDS results suggest that the stir behavior of tool successfully prohibits the formation of heavy IMC layer at the interface providing a fresh interface between Mg and steel, which promotes the formation of diffusion joint with a thin interface.

4. Discussion

The present experimental results reveal that the tool geometry has a significant effect on the evolution of microstructure and mechanical properties of magnesium alloy and steel lap joints. As we know, there are two main factors controlling the joining performance for solid-state bonded joint of dissimilar metals [21]. One is the intimate contact between dissimilar materials, and the other is the microstructure, particularly the formation of intermetallic compounds. In our experiment, the surface of steel does not get any surface treatment before welding. No fresh metal surface is exposed before welding so that there is no intimate contact between magnesium alloy and steel. For brushed finish steel joints welded using the 1.5-mm-length probe, there are lots of concavities on the rough surface of steel. The magnesium alloy is pushed into these concavities during FSW. Magnesium alloy and steel are joined through mechanical bonding. Therefore, brushed finish steel joints do not exhibit considerable fracture load. When the 1.8-mm-length probe is used, the tool is inserted in the lower steel side and the stir behavior of tool successfully provides a fresh interface between Mg and steel, which promotes the formation of diffusion joint with a thin interface. Therefore, the joints welded using the 1.8-mm-length probe exhibit considerable fracture load.

However, for zinc coated steel joints, the joints welded using the 1.5-mm-length probe exhibit considerable failure load compared with the brush finished steel joints. Obviously, the presence of zinc coat significantly improves the weldability of magnesium alloy and steel. As we know, the metal in the lap interface undergoes the synthetic effect of the thermal cycle and the mechanical cycle during FSW because of the action of friction, stir and extrusion of the tool. Thus, high temperature and high pressure are generated at the interface. Welding heat cycle histories test results show that the peak temperature in the center of joining interface is about 520 °C, higher than those of Zn melting point and Mg–Zn eutectic point (420 °C and 339 °C, respectively.), which results in the formation of a liquid phase. High temperature firstly leads to the melting of zinc coat and high pressure simultaneously results in the rupture of surface oxide films at both sheets surface, which promotes the formation of low melting Mg–Zn eutectic products. High pressure then forces the liquid Mg–Zn eutectic reaction products with broken oxide films and surface contaminants far away from the weld center, which spread along the interface till pile into the natural clearance between two sheets. In this way, the fresh interfaces are exposed and tightly extruded together after the liquid phase is pushed out. Elements mutual diffusion of Mg/Fe and Al/Fe occurs, which leads to the formation of a new IMC of Fe_4Al_{13} at the lap interface. Therefore, the joints welded using the 1.5-mm-length probe exhibit considerable failure load. In contrast, when the 1.8-mm-length probe is used, the failure loads of the joints do not show a satisfied value as expected because of void defect in the SZ. The formation of void defect can be explained due to the immixture of the low melting point liquid phase in the SZ arising from the synthetic effect of high temperature and the long probe. The presence of liquid phase leads to the formation of void defect. The defects act as a crack initiation site during tensile test.

Therefore, the joints fracture at the defect location and the failure loads of the joints do not show a satisfied value as expected.

5. Conclusions

AZ31 magnesium alloy and two kinds of steels (zinc coated steel and brushed finish steel) were lap welded using friction stir welding technology. The effect of tool geometry on microstructure and mechanical properties of the joints was studied and the following conclusions can be drawn.

1. For brushed finish steel joints, the failure loads of the joints increased significantly with the increasing probe length. The joints welded using a 1.8-mm-length probe fractured at the stir zone of magnesium alloy side while those welded using a 1.5-mm-length probe fractured at the joining interface. The microstructure at the joining interface varied significantly with the probe length. Magnesium alloy and steel were joined through mechanical bonding when the tool probe length is 1.5 mm. When the 1.8-mm-length probe was used, the tool was inserted in the lower side of steel and the stir behavior of tool successfully provided a fresh interface between AZ31 Mg alloy and steel, which promoted the formation of diffusion joint with a thin interface.
2. For zinc coated steel joints, the increase of the probe length did not significantly improve the tensile strength of the zinc coated steel joints because of void defect in the stir zone. The short probe contributed to defect-free joints and high-strength joints.

Acknowledgments

The authors are very grateful to Mr. Haruki Shingo for his contributory assistance. This work is supported by KAKENHI (17206074), Japan.

References

[1] Mao HK, Bell PM. Equations of state of MgO and xi Fe under static pressure conditions. J Geophys Res 1979;84:4533–6.
[2] Thomas WM, Nicholas ED, Needham JC, Murch MG, Templesmith P, Dawes CJ. GB Patent Application No. 9125978.8; December 1991.
[3] Park SHC, Sato YS, Kokawa H. Effect of micro-texture on fracture location in friction stir weld of Mg alloy AZ61 during tensile test. Scripta Mater 2003;49:161–6.
[4] Zhang D, Suzuki M, Maruyama K. Microstructural evolution of a heat-resistant magnesium alloy due to friction stir welding. Scripta Mater 2005;52:899–903.
[5] Feng AH, Ma ZY. Enhanced mechanical properties of Mg–Al–Zn cast alloy via friction stir processing. Scripta Mater 2007;56:397–400.
[6] Chang CI, Lee CJ, Huang JC. Relationship between grain size and Zener–Holloman parameter during friction stir processing in AZ31 Mg alloys. Scripta Mater 2004;51:509–14.
[7] Woo W, Choo H, Brown DW, Liaw PK, Feng Z. Texture variation and its influence on the tensile behavior of a friction-stir processed magnesium alloy. Scripta Mater 2006;54:1859–64.
[8] Reynolds AP, Tang W, Gnaupel-herold T, Prask H. Structure, properties, and residual stress of 304L stainless steel friction stir welds. Scripta Mater 2003;48:1289–94.
[9] Sorensen CD, Nelson TW, Packer SM. Tool material testing for FSW of high-temperature alloys. In: Proceedings of the third international symposium on friction stir welding, Kobe, Japan; 2001 [CD-ROM].
[10] Cui L, Fujii H, Tsuji N, Nogi K. Friction stir welding of a high carbon steel. Scripta Mater 2007;56:637–40.
[11] Fujii H, Cui L, Tsuji N, Maeda M, Nakata K, Nogi K. Friction stir welding of carbon steels. Mater Sci Eng A 2006;429:50–7.
[12] Thomas WM, Threadgill PL, Nicholas ED. Feasibility of friction stir welding steel. Sci Technol Weld Joining 1999;6:365–72.
[13] Lienert Jr TJ, Stellwag WL, Grimmett BB, Warke RW. Friction stir welding studies on mild steel. Weld J 2003;82:s1–9.
[14] Sato YS, Nelson TW, Sterling CJ, Steel RJ, Pettersson CO. Microstructure and mechanical properties of friction stir welded SAF 2507 super duplex stainless steel. Mater Sci Eng A 2005;397:376–84.
[15] Sato YS, Yamanoi H, Kokawa H, Furuhara T. Microstructural evolution of ultrahigh carbon steel during friction stir welding. Scripta Mater 2007;57:557–60.
[16] Watanabe T, Kagiya K, Yanagisawa A, Tanabe H. Solid state welding of steel and magnesium alloy using a rotating pin – solid state welding of dissimilar metals using a rotating pin. Quart J Jpn Weld Soc 2006;24:108–15.
[17] Zhao YH, Lin SB, Wu L, Qu FX. The influence of pin geometry on bonding and mechanical properties in friction stir weld 2014 Al alloy. Mater Lett 2005;59:2948–52.
[18] Fujii H, Cui L, Maeda M, Nogi K. Effect of tool shape on mechanical properties and microstructure of friction stir welded aluminum alloys. Mater Sci Eng A 2006;419:25–31.
[19] Tozaki Y, Uematsu Y, Tokaji K. Effect of tool geometry on microstructure and static strength in friction stir spot welded aluminium alloys. Int J Mach Tools Manuf 2007;47:2230–6.
[20] Elangovan K, Balasubramanian V. Influences of tool pin profile and tool shoulder diameter on the formation of friction stir processing zone in AA6061 aluminium alloy. Mater Des 2008;29:362–73.
[21] Kobayashi H, Nishimoto K, Ikeuchi K. Introduction to joining engineering of materials. Sampo 2002:182–8.